

# Transverse Single Spin Asymmetry of Electromagnetic Jets for Inclusive and Diffractive Processes at Forward Rapidity in $p^\uparrow + p$ Collisions at STAR\*

XILIN LIANG, FOR THE STAR COLLABORATION

UNIVERSITY OF CALIFORNIA, RIVERSIDE

*Received December 9, 2024*

We present the transverse single-spin asymmetry,  $A_N$ , for the electromagnetic jets (EM-jets) at forward rapidity in inclusive and diffractive processes in transversely polarized  $p^\uparrow + p$  collisions at  $\sqrt{s} = 200$  GeV at STAR. The inclusive EM-jet  $A_N$  is studied as functions of EM-jet transverse momentum and longitudinal momentum fraction, in different ranges of EM-jet energy and photon multiplicity. The  $A_N$  for single diffractive process and rapidity gap event, with a focus on photon multiplicity dependence, is also examined. A direct comparison of  $A_N$  from inclusive process, single diffractive process and rapidity gap events shows consistency within uncertainties. Furthermore, a non-zero  $A_N$  from semi-exclusive process is observed. These findings suggest that diffractive EM-jets do not contribute to the large  $A_N$  observed in the inclusive process at 200 GeV. Finally, we discuss the opportunities for the EM-jet  $A_N$  in inclusive and diffractive processes at  $\sqrt{s} = 510$  GeV.

## 1. Introduction

Transverse single-spin asymmetry ( $A_N$ ), also known as left-right asymmetry, refers to the azimuthal asymmetry in particle production relative to the plane defined by the momentum and spin directions of the polarized beam. In early predictions based on perturbative Quantum Chromodynamics (pQCD), this asymmetry was predicted to be nearly zero in hard scattering processes [1]. However, a large asymmetry has been observed in charged- and neutral-hadron productions from polarized hadron-hadron collisions [2, 3, 4, 5, 6]. Two major theoretical frameworks were developed to provide potential explanations for such sizeable asymmetry: the

---

\* Presented at “Diffraction and Low- $x$  2024”, Trabia (Palermo, Italy), September 8-14, 2024.

transverse-momentum dependent (TMD) formalism and the twist-3 factorization scheme. The TMD formalism introduces contributions from the initial-state quark and gluon Sivers functions and/or the final-state Collins fragmentation functions [7, 8]. The twist-3 factorization scheme involves contributions from the quark-gluon or gluon-gluon correlations and fragmentation functions [9]. Additionally, recent studies from STAR hinted that a large contribution to the observed asymmetry may come from diffractive processes [6].

The Relativistic Heavy Ion Collider (RHIC) is the only polarized proton-proton collider in the world. It can provide transversely or longitudinally polarized proton-proton collisions at  $\sqrt{s} = 200$  and 500/510 GeV. The STAR experiment, located at one of the collision points at RHIC, collected high-luminosity data with transversely polarized  $p^\uparrow + p$  collisions at  $\sqrt{s} = 200$  GeV and 510 GeV in 2015 and 2017, respectively. The average beam polarizations for these datasets are about 57% and 55%, with integrated luminosities of about  $52 \text{ pb}^{-1}$  and  $350 \text{ pb}^{-1}$ , respectively.

## 2. Multi-dimensional inclusive EM-jet $A_N$ for $p^\uparrow + p$ collisions at $\sqrt{s} = 200$ GeV

The Forward Meson Spectrometer (FMS) is the electromagnetic calorimeter which covers a pseudorapidity range of 2.6 to 4.2 with full azimuthal coverage at STAR [10]. The electromagnetic jets (EM-jets) are the jets reconstructed using only photons from the FMS. Details of the EM-jet reconstruction and correction can be found in [11].

The cross-ratio method was used to extract the  $A_N$ , with detailed explanations provided in [11]. The left panel of Fig. 1 shows the preliminary plot for the multi-dimensional study of inclusive EM-jet  $A_N$  at  $\sqrt{s} = 200$  GeV as a function of  $p_T$ , measured in three different regions of EM-jet energy ( $E_{jet}^{EM}$ ) and three cases of photon multiplicity ( $n_\gamma$ , number of photons inside the EM-jet). For EM-jets with  $x_F > 0$ , where  $x_F$  denotes the longitudinal momentum fraction,  $A_N$  decreases with photon multiplicity increases, with the largest  $A_N$  observed for EM-jets consisting of only 1- or 2- photons. Furthermore, the observed  $A_N$  is consistent with zero for  $x_F < 0$ .

The right panel of Fig. 1 presents preliminary results for the inclusive EM-jet  $A_N$  as a function of  $x_F$ , for different cases of the EM-jet photon multiplicity. They show that the  $A_N$  grows with  $x_F$  regardless of photon multiplicity, and the  $A_N$  for EM-jet for the case of 1- or 2- photon multiplicity is the largest. These results indicate a potential non-trivial contribution to the large  $A_N$  from diffractive processes, which motivates further exploration of the diffractive EM-jet  $A_N$ .

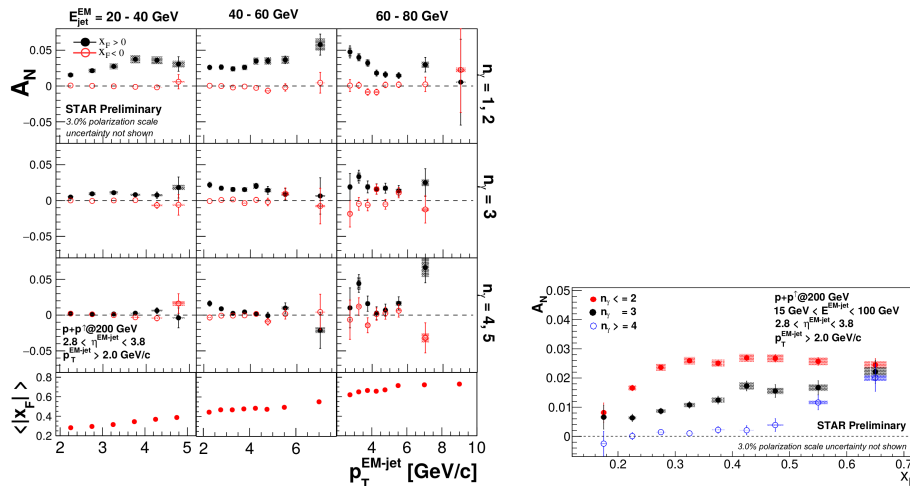


Fig. 1: (left)  $A_N$  of inclusive EM-jets at  $\sqrt{s} = 200$  GeV as a function of  $p_T$  sorted by three cases of EM-jet photon multiplicity and three energy bins. The lowermost panels display the average  $x_F$  values corresponding to each  $p_T$  bin. The black solid points represent the  $A_N$  values for  $x_F > 0$  and the red hollow points depict the  $A_N$  values for  $x_F < 0$ . (right) Inclusive EM-jet  $A_N$  as a function of  $x_F$  at  $\sqrt{s} = 200$  GeV for three cases:  $n_\gamma \leq 2$ ,  $n_\gamma = 3$ ,  $n_\gamma \geq 4$ .

### 3. Diffractive EM-jet $A_N$ for $p^\uparrow + p$ collisions at $\sqrt{s} = 200$ GeV

#### 3.1. Single diffractive EM-jet $A_N$

The single diffractive process requires detecting only one EM-jet at FMS and only one proton at the opposite side (east side) Roman Pot (RP). The RP detectors are designed to detect slightly-scattered protons in close proximity to the beamline [12]. The detected proton for the single diffractive process originates from the unpolarized proton beam. In addition, the rapidity gap, characteristic of the single diffractive process, is determined by a veto on the east side Beam-Beam Counter (BBC) [13]. The east side BBC is located between the FMS and the east side RP. It covers the pseudorapidity range of about three units,  $-5 < \eta < -2.1$ , which can satisfy the rapidity gap requirement of the diffractive process.

The left panel of Fig. 2 shows the preliminary plot for the single diffractive EM-jet  $A_N$  as a function of  $x_F$  categorized by photon multiplicity. For  $x_F > 0$ , the non-zero single diffractive EM-jet  $A_N$  value is found for both the combined photon multiplicity and EM-jets containing one or two photons. Furthermore, the  $A_N$  for EM-jets with one or two photons is much larger than for EM-jets with three or more photons.

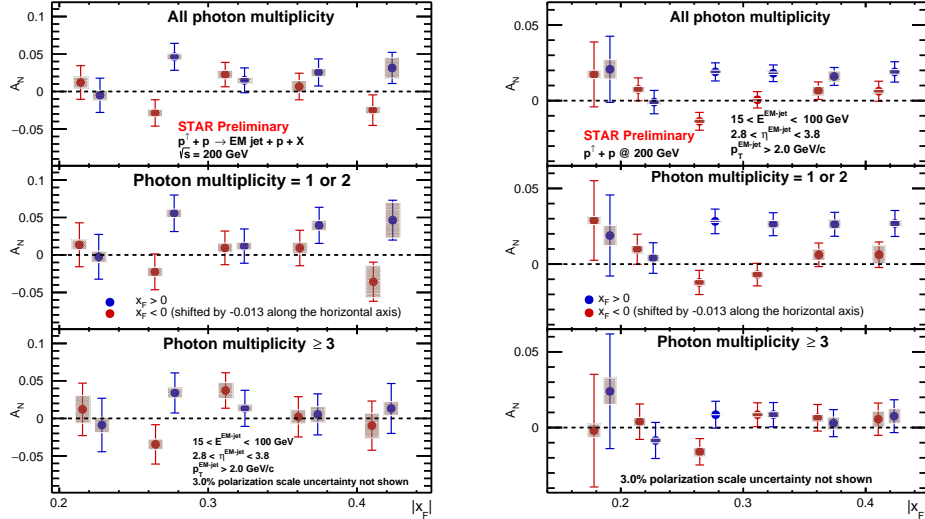


Fig. 2:  $A_N$  of single diffractive process (left) and rapidity gap events (right) EM-jet at  $\sqrt{s} = 200$  GeV for three photon multiplicity cases: all photon multiplicity(top), photon multiplicity  $\leq 2$  (middle), photon multiplicity  $\geq 3$  (bottom). The blue points represent the  $A_N$  values for  $x_F > 0$  and the red points depict the  $A_N$  values for  $x_F < 0$ .

### 3.2. Rapidity gap event EM-jet $A_N$

The set of events described in Sec. 3.1 with the proton tagged by east side RP represents only a small fraction of the real single diffractive events due to the limited acceptance of the RP detectors. To broaden the analysis, we also consider a category of events with only one EM-jet in the FMS and a veto on the east BBC without any requirement in RP. These are termed Rapidity Gap (RG) events, as the BBC veto still ensures a rapidity gap. Approximately 70% of the RG events are the real single diffractive process events. The right panel of Fig. 2 presents the preliminary results of the EM-jet  $A_N$  for the RG events as functions of  $x_F$  and photon multiplicity. It shows that the size of the EM-jet  $A_N$  for the RG events is similar to that of the inclusive events showing in Fig. 1. Additionally, the  $A_N$  is the largest for EM-jets with 1- or 2- photon multiplicity.

To investigate the contribution of single diffractive  $A_N$  to the inclusive  $A_N$ , a direct comparison of  $A_N$  for inclusive events, single diffractive events, RG events is shown in the left panel of Fig. 3. This comparison reveals that the  $A_N$  of these three processes are consistent within uncertainty. The diffractive processes constitute only a small fraction of the total inclusive cross section in the forward regime. Thus, this comparison provides evidence

that the large inclusive  $A_N$  cannot be attributed to the diffractive processes.

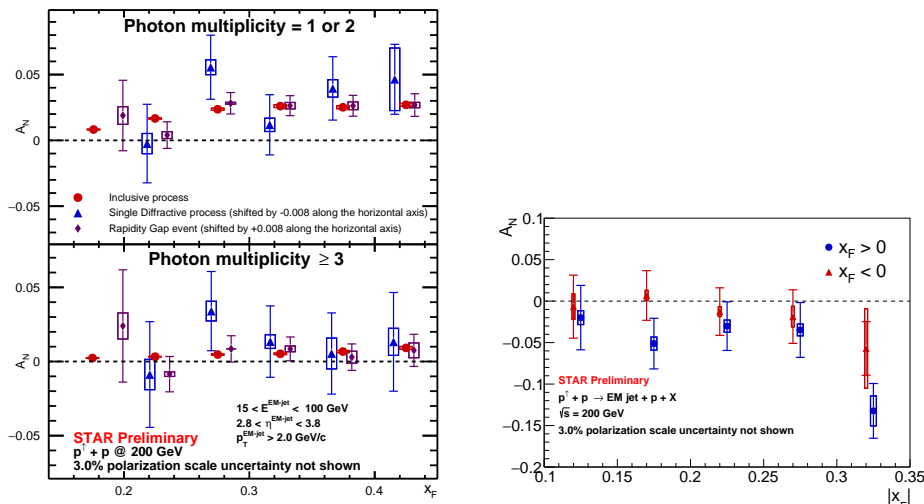


Fig. 3: (Left) Comparison of EM-jet  $A_N$  in inclusive process (red), single diffractive process (blue) and rapidity gap event (purple) at  $\sqrt{s} = 200$  GeV. (Right) EM-jet  $A_N$  for the semi-exclusive process as a function of  $x_F$  at  $\sqrt{s} = 200$  GeV. The blue points represent  $x_F > 0$ , while the red points represent  $x_F < 0$  with a constant shift of  $-0.005$  along the  $x$ -axis for clarity. The rightmost points correspond to  $0.3 < |x_F| < 0.45$ .

### 3.3. Semi-exclusive EM-jet $A_N$

The semi-exclusive process requires the detection of only one EM-jet at the FMS and only one proton, originating from the polarized proton beam, tagged by the west side RP. Additionally, the following constraint on the sum of energy of EM-jet in FMS and the west-site proton is applied: it needs to be equal to the beam energy, within the resolution. As the rapidity gap between the EM-jet and the west side proton is insufficient to meet the criteria for the diffractive process, this process is termed semi-exclusive process.

The right panel of Fig. 3 presents the preliminary results for semi-exclusive EM-jet  $A_N$  as a function of  $x_F$ . A non-zero  $A_N$  with a combined significance of  $> 3\sigma$  is observed for EM-jets with  $x_F > 0$ ; while the  $A_N$  for EM-jets with  $x_F < 0$  remains consistent with zero. Interestingly, the sign of  $A_N$  with  $x_F > 0$  is negative, which is different from the positive  $A_N$  observed in the inclusive process, as shown in Fig. 1. Further theories are needed to understand such different sign.

#### 4. Conclusion and outlook

In this study, we explore the multi-dimensional analyses on the EM-jet  $A_N$  for the inclusive process, single diffractive process, rapidity gap event and semi-exclusive process in  $p^\uparrow + p$  collisions at  $\sqrt{s} = 200$  GeV at STAR. The photon multiplicity-dependent EM-jet  $A_N$  is observed for EM-jet in the inclusive process, single diffractive process and rapidity gap events, with the largest  $A_N$  observed for EM-jets consisting of one or two photons. The EM-jet  $A_N$  increase with increasing  $x_F$  in the inclusive process. A non-zero  $A_N$  is observed for the EM-jet with one or two photons in the single diffractive process. However, the  $A_N$  values for the inclusive process, single diffractive process and the rapidity gap event are consistent with each other within uncertainty. The semi-exclusive EM-jet shows the non-zero  $A_N$  with a negative sign. These results indicate that the diffractive EM-jet  $A_N$  can not provide evidence to contribute to the large  $A_N$  in inclusive process at 200 GeV.

Analyses of inclusive and diffractive EM-jet  $A_N$  in  $p^\uparrow + p$  collisions at  $\sqrt{s} = 510$  GeV at STAR are in progress. Compared to the measurements in 200 GeV dataset, this higher-luminosity dataset allows the higher-statistical measurements of  $A_N$  in these processes, especially it enables studying  $A_N$  for single diffractive process at lower  $x_F$  region.

#### REFERENCES

- [1] G. L. Kane, J. Pumplin, and W. Repko. Phys. Rev. Lett. 41, 1689 (1978)
- [2] D.L. Adams *et al.*, Phys. Lett. B 261, 201(1991)
- [3] B. I. Abelev *et al.* (STAR Collaboration), Phys. Rev. Lett. 101, 222001(2008)
- [4] A. Adare *et al.* Phys. Rev. D 90, 012006 (2014)
- [5] E.C. Aschenauer *et al.*, arXiv:1602.03922
- [6] J. Adam *et al.* (STAR Collaboration), Phys. Rev. D 103, 092009 (2021)
- [7] D. Sivers, Phys. Rev. D 41, 83 (1990)
- [8] J. Collins, Nucl Phys B 396 (1993) 161
- [9] J.W. Qiu and G. Sterman, Phys. Rev. Lett. 67 2264 (1991)
- [10] J. Adam *et al.* (STAR Collaboration), Phys. Rev. D 98, 032013 (2018)
- [11] X. Liang (STAR Collaboration) 10.5281/zenodo.7236716
- [12] J. Adam *et al.* (STAR Collaboration), Phys. Lett. B 808 (2020) 135663
- [13] K. H. Ackermann *et al.* (STAR Collaboration), Nucl. Instrum. Meth. A 499, 624-632 (2003).